The effect of manufacturing mismatch on energy production for large-scale photovoltaic plants

A. Massi Pavan[(1)], A. Tessarolo[(1)], N. Barbini[(1)], A. Mellit[(2,3)] and V. Lughi[(1)]

[(1)] Department of Engineering and Architecture, University of Trieste, Via A. Valerio 6/A – 34127 Trieste, Italy

[(2)] Faculty of Sciences Technology, Renewable energy laboratory, Jijel University, Ouled-aissa, P. O. Box 98, Jijel 18000, Algeria

[(3)] International Centre for theoretical physics (ICTP), Strada Costieria, 11-34151,Trieste, Italy

Abstract

In the literature, the effect of the mismatch due to manufacturing tolerances on PV plant productivity has been investigated under the hypothesis of plant operation in Standard Test Conditions (STC). In this paper, mismatch impacts are evaluated in more realistic terms taking into account various possible operating conditions. Results are illustrated through the study case of a 1 MWp solar park for which module datasheets as well as flash test data are available. The plant production is evaluated assuming operating conditions that comply with the European efficiency standards. It is shown how the effect of a given mismatch on the annual productivity estimation can significantly change depending on the operating conditions.

Keywords—Photovoltaic power system; large-scale photovoltaic plant; manufacturing mismatch losses; negative mismatch losses; performance.

Corresponding author: Dr. A. Massi Pavan, Email. apavan@units.it

1. Introduction

With reference to Fig. 1, the photovoltaic (PV) worldwide market is continuing its exponential growth (Solar energy report, 2014) with a cumulative power with more than 132GWp at the end of 2013. In 2013, photovoltaics was still the technology exhibiting the highest growth rate in the renewable power sector (REN 21, 2012). In Italy, which is the third worldwide country for PV installations with more than 18MWp installed (http://www.gse.it), this source guarantees more than 10% of the consumed electricity (http://www.terna.it).

The transition from the era of subsidies (e.g. the Italian policy of incentives has recently ended) to that of grid parity, which has been attained in many locations under a broad range of conditions (Massi Pavan and Lughi, 2012; Massi Pavan and Lughi, 2013), represents the passage from childhood to maturity for this solar technology. As the yield of PV plants plays a fundamental role in the determination of grid parity, a more and more accurate calculation of PV plant appears necessary. A phenomenon that must be taken into account for this purpose relates to the power losses that arise due to mismatch, i.e. when modules with different current-voltage characteristics (I-V characteristics) are interconnected (Luque A., Hegedus, 2006). The mismatch effect of the manufacturing tolerances was investigated by (Chamberlin et al. 1995); it has been shown that no discernible difference was observed in the maximum output power from parallel string arrays and series block arrays. A statistical approach based on Monte-Carlo technique has been developed in (Iannone et al., 98) to analyze the electrical mismatch of a 100kWp PV standard unit generator. The manufacturing I-V mismatch calculated at Standard Test Conditions (STC) was 0.56% (Spertino and Akilimali, 2009). In (Kaushika and Rai, 2007), the authors showed that with an appropriate series/parallel connection of PV modules, the mismatch losses are in the range [0.4 - 2.4%]. A comprehensive method for evaluating energy loss due to shading effect of a Grid-Connected Building Integrated PV system is presented by (Drif et al., 2012), it has been shown that, the results showed that loss of energy is 1.79 kWh/day, which corresponds to a shading factor of 14.4%. With respect to (Wurster and Schubert, 2014), simulation results demonstrate that photovoltaic systems with strings of different length in parallel to several others which have an equal module count renders mismatch losses below 1% for most configurations. It has been also proven that, for configurations where one string is one module shorter than the others, the mismatch losses fall below 0.5%. As reported in (Lorente et al., 2014) a small array of 40 modules has a negligible loss while 320 modules array has a more significant mismatch

loss at about 0.23% of the nominal power. It has been also shown that, module ordering decreases this value to 0.10% and increases the calculated energy.

However, STC represent only a reference needed to rate the power of a PV device, but they hardly occur during the operation of a real PV plant. Furthermore, the purpose of this work is to investigate how the losses due to manufacturing tolerance change depending on environmental conditions. In particular, evaluations are performed for illustrative purposes assuming some plant operating conditions that have a larger probability to happen. Such conditions are identified by the International Electrotechnical Commission in the IEC 61724 Standard in order to define European efficiency values (IEC 61724).

The proposed investigations are conducted on a sample 1 MWp solar plant for which PV module datasheet and flash test data are known. Plant productivity evaluations are based on the empirical model introduced in (Massi Pavan et al., 2014a) and experimentally validated at maximum power point in (Massi Pavan et al., 2014b). In order to calculate the mismatch losses, the yield of the PV plant is calculated in two ways: (i) assuming that all the PV plant modules are identical and share the same electrical parameters provided in the datasheet; (ii) based on the data extrapolated from the flash tests referring to each module. The mismatch losses are then obtained as the difference of the yields computed in the two mentioned ways.

This work is organized as follows: in the next Section, the empirical model of single module is introduced. In Section 3 the model is extended for the purpose of studying a complete field including multiple interconnected modules In Section 4 the case study is introduced, whereas results are discussed in Section 5. Finally, the conclusions are given in Section 6.

2. Empirical model

The advantage of the empirical model presented in (Massi Pavan et al., 2014a) is that the electrical parameters listed in the datasheets or in the flash tests of any PV module are sufficient to describe the behavior of the module itself. For this reason, such empirical model has chosen hereinafter. For a single PV module, the following equations are then used to relate its current I and voltage:

$$I = I_L + z \cdot \Delta T - \frac{e^{m \cdot [V - w \cdot \Delta T]} - 1}{e^m - 1} \qquad (1)$$

or, equivalently:

$$V = \log\left\{\left[e^{m} - 1\right] \cdot \left[I_L - I + z \cdot \Delta T\right] + 1\right\} + w \cdot \Delta T \qquad (2)$$

where I [p.u.] is the per unit current referred to the short circuit current I_{sc} [A] at STC, I_L [p.u.] is the per unit irradiance referred to 1.000W/m^2, T_c [°C] is the solar cell temperature, m [ ] is an exponential factor, V [p.u.] is the per unit voltage referred to the open circuit voltage V_{oc} [V] at STC, z [1/°C] is the current-temperature coefficient referred to the short circuit current at STC ($z = Z/I_{sc}$, where Z [A/°C] is the current-temperature coefficient from the datasheet of the considered PV module) and w [1/°C] is the voltage-temperature coefficient referred to the open circuit voltage at STC ($w = W/V_{oc}$, where W [V/°C] is the voltage-temperature coefficient from the datasheet of the considered PV module), $\Delta T = (T_C - 25)$ [K] is the temperature deviation from the standard temperature of 25°C.

In order to evaluate the exponential factor m, two steps are needed: firstly the fill factor for a given irradiance I_L and cell temperature T_c is computed as described in (Massi Pavan et al., 2014a); secondly, m is determined such that the same fill factor results from (1) as well.

3. Model extension for multiple modules

In this Section, the empirical model recalled in Section 2 for a single module is extended to the case of a PV field composed of N parallel strings, each including M series-connected modules. The procedure is first described in analytical terms and then its numerical implementation is reported.

3.1.Analytical description

If all the PV modules had the same exponential factor m, STC open circuit voltage V_{OC}, and STC short circuit current I_{SC}, the following equations could be derived from (1) for the j-th string:

$$\begin{aligned} V_j &= MV \quad \forall j = 1 \ldots N \\ I_j &= I, \quad \forall j = 1 \ldots N \end{aligned} \qquad (3)$$

and for the whole field:

$$\begin{aligned} V_{field} &= MV \\ I_{field} &= NI \end{aligned} \qquad (4)$$

where V_j, I_j are the voltage and currents of the j-th string in per unit of V_{BASE} = V_{OC} and I_{BASE} = I_{SC}, respectively, and V_{field} and I_{field} are the voltage and current of the whole field with respect to the same base quantities.

When the PV modules feature different electrical parameters voltages and currents must be brought to a common base as follows:

$$\begin{aligned} I_{i,j} &= I(i,j)\cdot\frac{I_{SC}(i,j)}{I_{BASE}} \\ V_{i,j} &= V(i,j)\cdot\frac{V_{OC}(i,j)}{V_{BASE}} \end{aligned} \qquad (5)$$

where indices $i=1...M$ and $j=1...N$ refer to the i-th module of j-th string in the field, $I(i,j)$ and $V(i,j)$ are the dimensionless current and voltage referred to the short-circuit values $I_{SC}(i,j)$, $V_{OC}(i,j)$ obtained from the PV module flash tests, while $V_{i,j}$ and $I_{i,j}$ are per unit values referred to common bases I_{BASE} and V_{BASE} respectively equal to the short circuit current I_{SC} [A] and the open circuit voltage V_{OC} [V] obtained from the datasheet, which is the same for all the modules.

By substitution of (1) and (2) into (5) with the appropriate module indices, we obtain:

$$\begin{aligned} I_{i,j} &= \frac{I_{\mathrm{SC}}(i,j)}{I_{\mathrm{BASE}}}\left[I_L + z\cdot\Delta T - \frac{e^{m_{i,j}\cdot[V(i,j)-w\cdot\Delta T]}-1}{e^{m_{i,j}}-1}\right] \\ V_{i,j} &= \frac{V_{\mathrm{OC}}(i,j)}{V_{\mathrm{BASE}}}\frac{\log\left[\left(e^{m_{i,j}}-1\right)\cdot\left(I_L + z\cdot\Delta T - I(i,j)\right)+1\right]}{m_{i,j}} + w\cdot\Delta T \end{aligned} \qquad (6)$$

Therefore, the j-th string voltage and currents are obtained as follows:

$$\begin{aligned} I_j &= I_{i,j}, \quad \forall j = 1\ldots N \\ V_j &= \left\{\sum_{i=1}^{M}\frac{V_{OC}(i,j)}{m_{i,j}\cdot V_{BASE}}\log\left\{\left(e^{m_{i,j}}-1\right)\left(I_L - I_j + z\cdot\Delta T\right)+1\right\}\right\} + M\cdot w\Delta T \end{aligned} \qquad (7)$$

and, finally, for the whole field we have:

$$\begin{aligned} I_{field} &= \sum_{j=1}^{N} I_j \\ V_{field} &= V_j, \quad \forall j = 1\ldots N \end{aligned} \qquad (8)$$

where V_j [p.u.] is the voltage of the j-th string, I_j [p.u.] is the same current imposed through the M modules of the j-th string.

Equation (8) does not univocally determine the operating point of the field. This can be fixed by imposing that a maximum power P_{field} is being tracked by a suitable Maximum Power Point Tracker (MPPT) system, so that

$$\begin{cases} P_{field} = V_{field} \cdot I_{field} \\ \dfrac{\partial P_{field}}{\partial V_{field}} = 0 \end{cases} \qquad (9)$$

To consider the presence of by-pass diodes (mounted in parallel to each module) and blocking diodes (in series with each string), the calculated values of $V_{i,j}$ and I_j respectively are considered valid if positive otherwise they are imposed to be zero.

3.2.Numerical implementation

The numerical implementation of the method described Section in 3.1 is represented in Fig. 2 as a flow-chart. During the first step the parameters of equation 6 are fixed: z, w, I_{BASE}, V_{BASE} are assumed to be the same for all the PV modules and are from the data-sheet (Table 1); $V_{OC}(i,j)$ and $I_{SC}(i,j)$ are from the flash test of the considered (i,j) PV module; $m_{i,j}$ is numerically computed according to the procedure described in (Barbini et al., 2014) and (Massi Pavan et al., 2014a) for the different irradiances G and cell temperatures T (see Section 4.2). The second step calculates the produced power P_{field} as a function of the output voltage V_{field}. The power is calculated by means of the procedure detailed in the flow-chart shown in Fig. 3: for any j=1...N the algorithm numerically searches for the string current I_j such that the j-th string voltage given by equation 7 equals V_{field}. The resulting string currents I_j (j=1..N) are then summed to obtain the field current I_{field}, which is multiplied by the field voltage V_{field} to obtain the produced power P_{field}. The algorithm is repeated varying the voltage V_{field} so as to identify the global maximum of the function $P_{field}(V_{field})$.

4. Case study

In this Section, the model presented in Section 3 is applied to evaluate the yield of a real PV field of which the main characteristics are provided. Two cases will be considered for the same PV plant, i.e. the case where all the modules are identical and have the same electrical parameters specified in the data-sheet and the case where the PV modules are affected by a certain manufacturing mismatch. In the latter case, the electrical parameters of each module are obtained from the flash test and differ, in general, from those indicated in the data-sheet.

For the sake of simplicity, the two mentioned cases will be approached assuming to have two different PV modules, that will be next indicated as “Field 1” and “Field 2”, such that: “Field 1” is the real one

where all modules are different and characterized by their relevant flash tests; “Field 2” is the ideal one where all modules are identical and identified by their common data-sheet parameters.

4.1 Photovoltaic plant characteristics

With reference to Fig. 4, the considered 1MWp PV plant implements a centralized solution (Massi Pavan et al., 2007) and is composed of two sub-fields each connected to an inverter with a MPPT control. The proposed configuration, that is of the series-parallel (SP) type (Kaushika and Gautam, 2003; Shams El-Dein et al., 2013), is widely used by designers of large-scale solar parks. The output of the two inverters is connected to a double primary transformer (315V) interfaced to the medium voltage electrical grid operating at 20kV.

The PV modules constituting the two sub-fields are “Q.Pro G2 240” models produced by Q.Cells (http://www.qcells.com), featuring a multi-crystalline silicon technology; their electrical data are reported in Table 1.

Every sub-field is composed of 86 PV strings, each consisting of 24 “Q.Pro G2 240 PV” modules. The total number of PV modules is then 2×86×24=4128 and the nominal power of the PV generator is 990.72kWp.

Due to the unavoidable spread of the individual silicon cell electrical characteristics, the real power of the considered modules at STC is different from the nominal value of 240Wp and falls within a given power tolerance (typically ±5%). The 4128 PV modules considered here have been provided by the manufacturer along with the data resulting from flash tests, reporting the actual electrical parameters (power at STC, current and voltage at maximum power point, open circuit voltage and short circuit current) for each module. These data have been used in the present study in order to assess the manufacturing mismatch losses.

With reference to the STC power, Fig. 5 depicts the distribution of the considered stock of PV modules. The histogram has been obtained dividing the power range into 20 intervals and shows the number of occurrences for each of them.

4.2 Operating conditions assumed for simulations

In order to assess the impact of the manufacturing mismatch losses (i.e. that measured over an entire year of operation), the definition of European efficiency (IEC 61724) is taken into account. The latter is based on the definition of a number solar irradiance and temperature values and corresponding weights, which quantify the amount of energy produced for that irradiance and temperature. Table 2 reports the solar

irradiance, the corresponding cell temperature, and the weights for the operating conditions considered in this work.

It is worth noting that the calculation of the manufacturing mismatch losses based on different working conditions rather than on the only Standard Test Conditions is expected to lead to more accurate and realistic results. In fact, during the operation of a PV generator, the PV modules never operate at a solar irradiance of 1.000W/m^2 and at a cell temperature of 25°C.

The losses associated to the manufacturing mismatch are calculated as the difference (in percent) between two weighted values of the power. The first is the weighted power produced by PV "Field 1", where the electrical parameters from the flash test are considered for each module. The second is the weighted power produced by identical 4128 PV modules all operating at their maximum power point and characterized by the same electrical parameters taken from the PV module datasheet (PV "Field 2").

5. Results and Discussion

The model described in Section 3 is applied to "Field 1" and "Field 2", particularly using equations 3 and 4 for the latter and equations 5 and 9 for the former. Results are given in Tables 3 and 4 where the per unit values are referred to a base voltage of 37.20V, a base current of 8.45A and a base power of 314.44W. The tables show the maximum power produced by "Field 1" and "Field 2" in the different working conditions identified in Table 2.

As an example, Fig. 6 shows the per unit power-voltage characteristics of PV "Field 1" operating at four different working conditions.

The weighted power P_i (i =1, 2), respectively referring to "Field 1" and "Field 2", is calculated considering the weight factors reported in Table 2:

$$P_i = 0.03 \times P_{i,A} + 0.06 \times P_{i,B} + 0.10 \times P_{i,C} + 0.13 \times P_{i,D} + 0.48 \times P_{i,E} + 0.2 \times P_{i,F} \quad (10)$$

where, for example, $P_{1,A}$ is the maximum power produced by "Field 1" in the operating condition A.

Table 5 shows the losses due to the manufacturing mismatch for the different working conditions calculated as:

$$\varepsilon_k = \frac{P_{2,k} - P_{1,k}}{P_{2,k}} \times 100 \quad (11)$$

with k = A, B, …, F; furthermore, the overall mismatch loss resulting from weight application is shown in the last row of the table and is computed as:

$$\varepsilon = \frac{P_2 - P_1}{P_2} \times 100 \qquad (12)$$

With reference to Fig. 7, the manufacturing mismatch loss grows with solar irradiance. It is also shown that for irradiances smaller than 200W/m^2, the manufacturing mismatch losses are negative, which means that the mismatch brings a gain. The phenomenon is based on the considerations developed in (Barbini et al., 2014) and in (Massi Pavan et al., 2014a) in terms of fill factor. Here, the experimentally-proven equation 1 has been combined with the relationships given in (Luque and Hegedus, 2006) and (Markvart and Castaner, 2003) between the fill factor and the operating conditions of irradiance and cell temperature. The result is that the fill factor increases when the solar irradiance decreases, while it is much less affected by changes in the cell temperature. Such increase in the fill factor is not the same for all the PV modules: the ideal modules constituting "Field 2" exhibit a lower fill factor increase than the majority of the real ones constituting "Field 1", as exemplified by the case studies explained in (Barbini et al., 2014). This phenomenon physically accounts for the better performance of "Field 1" compared to "Field 2" at low irradiance values.

The above results show that there are two main kinds of non-idealities to be taken into account when predicting the productivity of a real PV plant:

1) the characteristics of each module are, in general, different from those declared in its datasheet;

2) the various modules constituting the PV plant have, in general, different characteristics.

In terms of impacts on PV plant productivity, the second non-ideality always leads to losses in a Series-Parallel connected field as it prevents each module to operate in its optimal operating conditions (Maximum Power Point), while the first can have an either positive or negative impact. The "sign" of the impact, as well as its magnitude, also depends on the operating conditions and on irradiance levels in particular, as discussed in (Barbini et al., 2014) and confirmed by the results shown in Fig. 7. In other words, the investigated case study shows that the different parameters of the PV modules (i.e. the parameters from the datasheet are different than the real ones coming from the flash test) can bring some benefits in terms of productivity at low irradiances.

6. Conclusions

In this work, the effects of manufacturing mismatch on energy production for large-scale PV plants have been investigated in regard to their dependency upon operating conditions.

As a study case, the mismatch losses have been assessed considering the electrical parameters from the flash tests of 4128 multi-crystalline PV modules forming a centralized 1MWp PV generator.

A number of operating conditions have been considered in accordance to the definition of European Efficiency to account for the various solar irradiances statistically occurring over a year. This approach has been proposed as an alternative to the conventional one where the PV plant is referred to the STC only. In particular, it has been shown that the losses calculated at STC give an overestimation of the manufacturing mismatch losses that occur in a real PV plant.

Furthermore, it is to be emphasized that, while the weighted loss is 0.21% and the one at STC is 0.35%, it has been shown that the manufacturing mismatch losses grow with the solar irradiance and can even be negative (i.e. the overall mismatch effect brings a gain) under a certain value of solar irradiance (in this case 200W/m^2).

In terms of power dispatching plans, the last mentioned result has never been considered before in the literature and can have an impact in predicting power produced by large-scale PV plants when operating in the early morning, in the evening or with cloudy sky.

Again, with reference to the estimation of the produced power, the technology of the considered PV modules is another key point for future studies. In fact, as shown in (Barbini et al., 2014), a difference between the real and the nominal fill factor can bring a benefit in terms of produced energy. This kind of mismatch, strongly dependent on the module technology, opposes its effect to the known mismatch losses due to a slight difference among modules regarding their maximum power point. It has been proven that the energy benefit can be such to prevail over the mismatch losses in low irradiance conditions.

Acknowledgements

Dr. Adel Mellit would like to thank the International Centre for Theoretical Physics (ICTP), Trieste (Italy) for providing the materials and computer facilities for performing part of the work made for the validation of the used model.

References

Barbini, N. Lughi V., Mellit A., Massi Pavan A., Tessarolo A., 2014. On the impact of photovoltaic module characterization on the prediction of PV plant productivity, Ecological Vehicles and Renewable Energies (EVER), 25-27.

Chamberlin C.E., Lehman P., Zoellick J., Pauletto G., 1995. Effects of mismatch losses in photovoltaic arrays, Sol Energy, 54, 165-171.

Drif M., Mellit A., Aguilera J., Pérez P.J., 2012. Comprehensive method for estimating energy losses due to shading of GC-BIPV systems using monitoring data. Sol Energy. 86, 2397-2404.

Iannone F., Noviello G., Sarno A.,1998. Monte Carlo techniques to analyse the electrical mismatch losses in large-scale photovoltaic generators, Sol. Energy 62, 85–92.

IEC 61724 – Photovoltaic system performance monitoring guidelines for measurement, data exchange and analysis.

Kaushika N. D., Rai A. K., 2007.An investigation of mismatch losses in solar photovoltaic cell networks. Energy, 32 ,755–759.

Kaushika N.D., Gautam N.K., 2003. Energy yield simulations of interconnected solar PV arrays. IEEE Transaction on Energy Conversion, 18,127-134.

Lorente G.G, Pedrazzi S., Zini G., Rosa A.D, Tartarini P., 2014. Mismatch losses in PV power plants, Solar Energy , 42–49

Luque A., Hegedus S. Handbook of photovoltaic science and engineering. New York, John Wiley and Sons Inc., page 951, 2006.

Markvart T., Castaner L. Photovoltaics Fundamentals and Applications. Elsevier Ltd., page 75, 2003.

Massi Pavan A., Castellan S., Quaia S., Roitti S., Sulligoi G., 2007.Power electronic conditioning systems for industrial photovoltaic fields: centralized or string inverters? IEEE International Conference on Clean Electrical Power, Capri, Italy, pp. 208-214.

Massi Pavan A., Lughi V, 2013. Grid parity in the Italian commercial and industrial electricity market, in Proc. of IEEE International Conference on Clean Electrical Power, Alghero, Italy, p. 332 – 335.

Massi Pavan A., Lughi V., 2012.Photovoltaics in Italy: toward grid parity in the residential electricity market, in Proc. of IEEE International Conference in Microelectronics, Algiers, Algeria, pp. 1-4.

Massi Pavan A., Mellit A., De Pieri D., and Lughi V., 2014a. A study on the mismatch effect due to the use of different photovoltaic modules classes in large-scale solar parks. Progress in Photovoltaics: Research and Applications, 22, 332-345.

Massi Pavan A., Mellit A., Lughi V., 2014b. Explicit empirical model for general photovoltaic devices: Experimental validation at maximum power point. Sol. Energy 101; 105-116.

Shams El-Dein M. Z., Kazerani M., Salama M. M. A., 2013.Optimal photovoltaic array reconfiguration to reduce partial shading losses. IEEE Transaction on sustainable energy, 4,145-153.

Spertino F., and Akilimali J. S., 2009. Are manufacturing I–V mismatch and reverse currents key factors in large photovoltaic arrays?. IEEE Transaction on Industrial Electrononics, 56,4520–4531.

Wurster T.S., Schubert M.B, 2014. Mismatch loss in photovoltaic systems, Sol. Energy 105 , 505–511

http://www.energystrategy.it, Solar energy report, MIP, 2014. Accessed on September 2014

http://www.ren21.nt, Renewables 2012. Global status report, REN 21. Accessed on October 2013
http://www.gse.it. Accessed on September 2014
http://www.terna.it. Accessed on September 2014
http://www.qcells.com. Accessed on October 2013

Table 1 Electrical parameters of the PV modules at STC (irradiance 1000W/m^2, cell temperature 25°C, solar spectrum AM1.5)

Nominal power P_n [W]	240
Short circuit current I_{sc} (I_{BASE}) [A]	8.45
Open circuit voltage V_{oc} (V_{BASE}) [V]	37.20
Current at maximum power point I_{mp} [A]	7.96
Voltage at maximum power point V_{mp} [V]	30.20
Current-temperature coefficient Z [A/°C]	0.0034
Voltage-temperature coefficient W [V/°C]	-0.11
Current-temperature coefficient z [1/°C]	4×10^{-4}
Voltage-temperature coefficient w [1/°C]	-0.0030
Series connected solar cells [ ]	60

Table 2 Solar irradiance and cell temperatures

Working Condition	Solar Irradiance [p.u. – W/m^2]	Cell Temperature [°C]	Weight
A	0.05 – 50	16.5	0.03
B	0.10 – 100	18.0	0.06

C	0.20 – 200	21.0	0.13
D	0.30 – 300	24.0	0.10
E	0.50 – 500	30.0	0.48
F	1.00 – 1000	45.0	0.20

Table 3

Power produced by PV field 1

Working Condition	Produced Power [p.u.]	Produced Power [kW]
A	147.76393	46.448
B	312.10922	98.108
C	637.91149	200.521
D	955.75345	300.431
E	1562.39523	491.120
F	2902.21394	912.281
STC	3140.67026	987.238
Weighted P_1	-	484.582

Table 4

Power produced by PV field 2

Working Condition	Produced Power [p.u.]	Produced Power [kW]
A	147.612256	46.400
B	311.864377	98.031
C	637.749210	200.470
D	956.021623	300.516

E	1564.48414	491.780
F	2913.73041	915.902
STC	3151.74652	990.720
Weighted P_2	-	485.623

Table 5

Mismatch losses at different working conditions

Working Condition	Loss [%]
A	-0.10
B	-0.08
C	-0.02
D	0.03
E	0.13
F	0.40
STC	0.35
Weighted	0.21

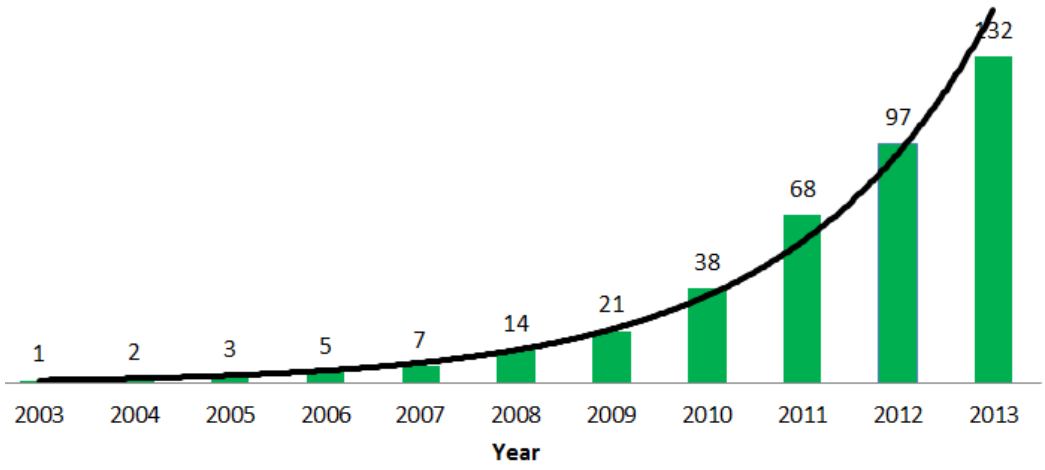

Fig.1.Worldwide cumulative installed power in GWp.

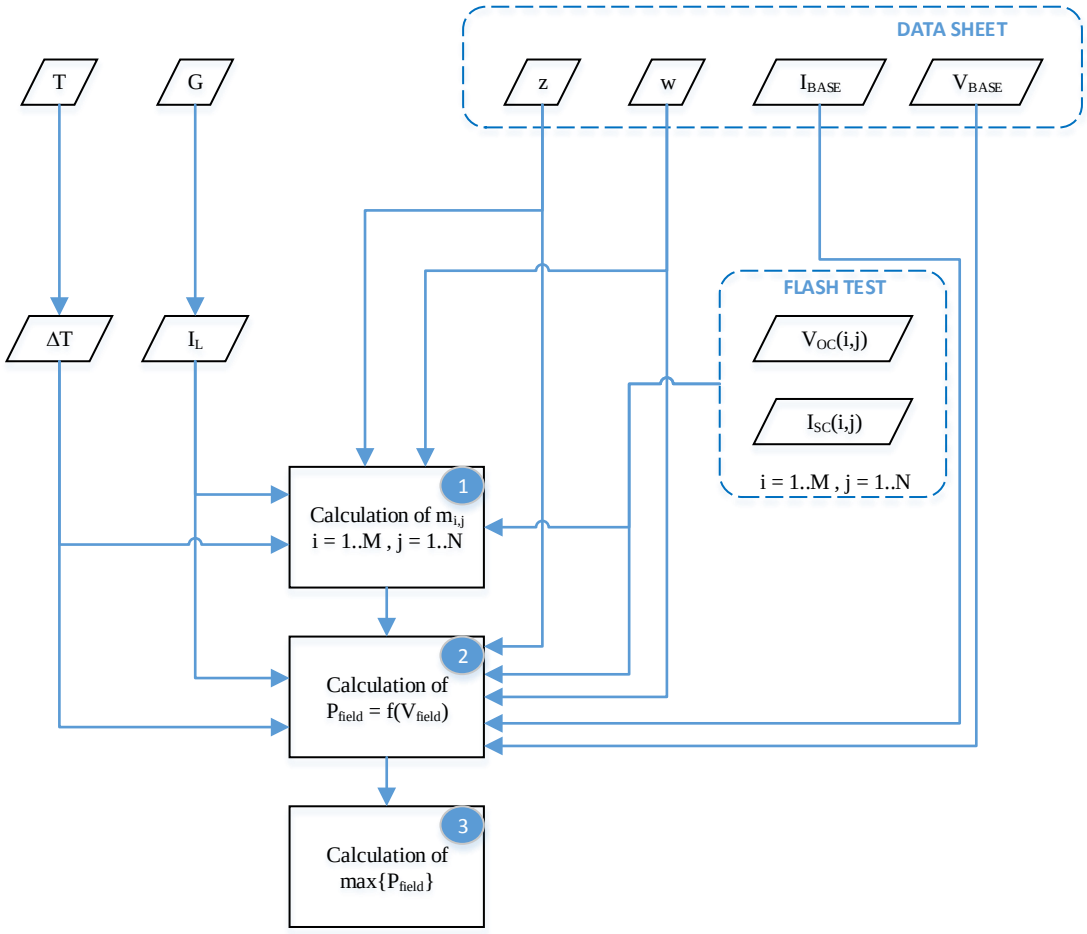

Fig. 2. Flow chart for the numerical computation of the maximum power produced by the PV field for any given irradiance G and temperature T

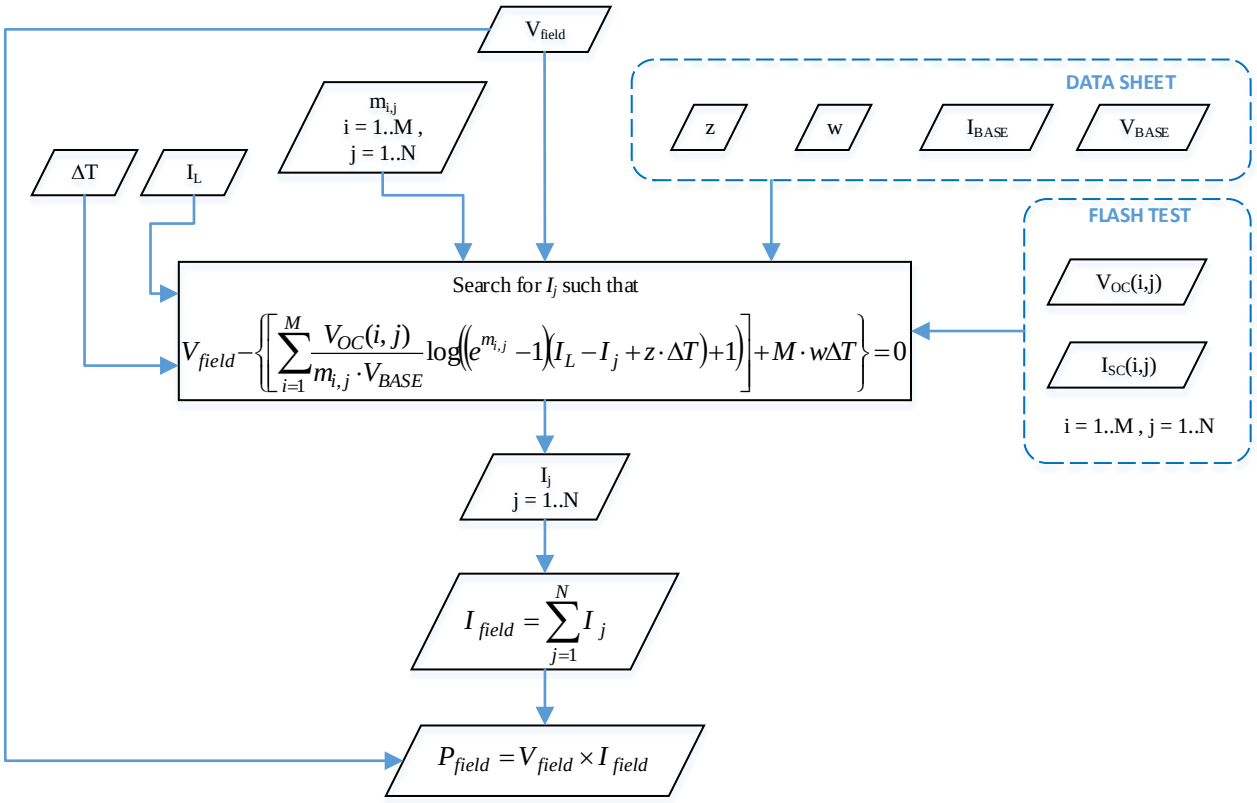

Fig. 3. Flow chart for the numerical computation of field power P_{field} as a function of the field voltage V_{field}

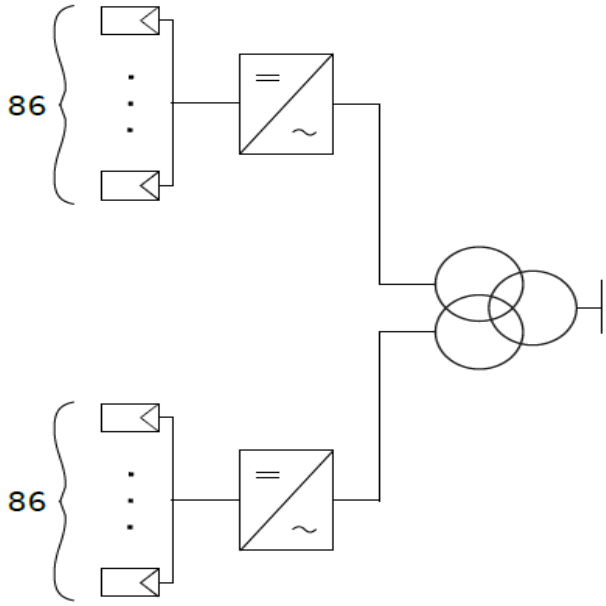

Fig.4. Electrical scheme of the considered PV plant.

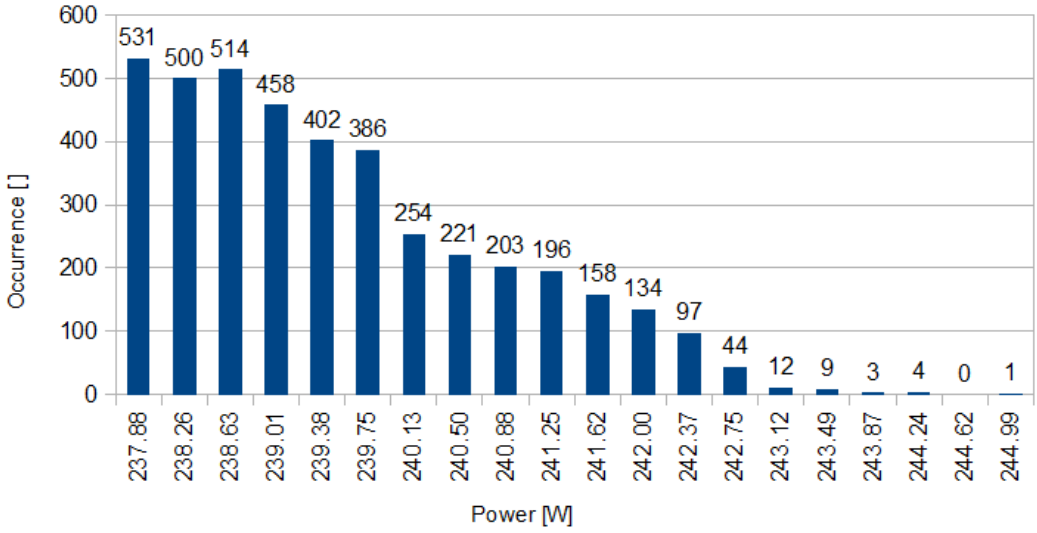

Fig.5. Distribution of the effective STC power of the considered PV modules.

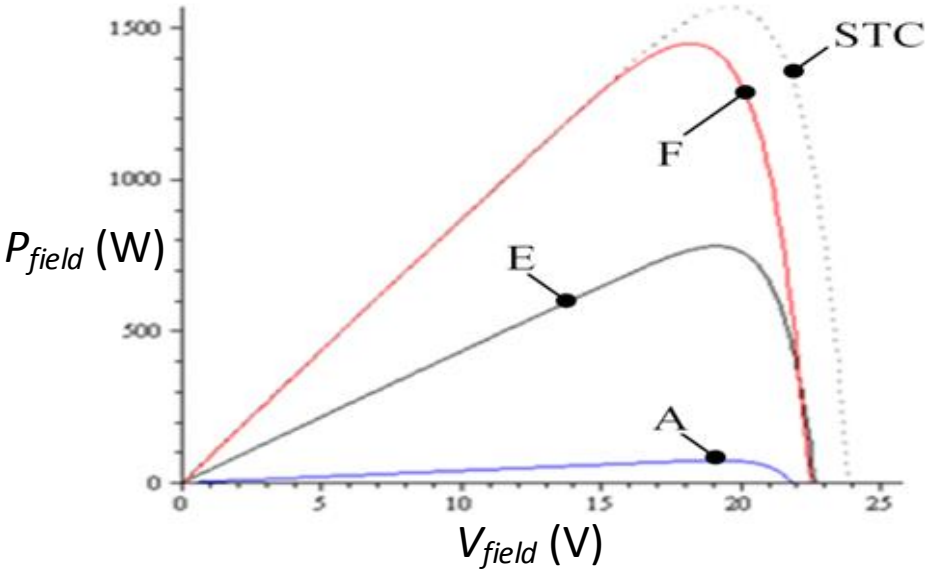

Fig.6. Per unit power-voltage characteristics for PV field 1 operating at different working conditions (see Table 2).

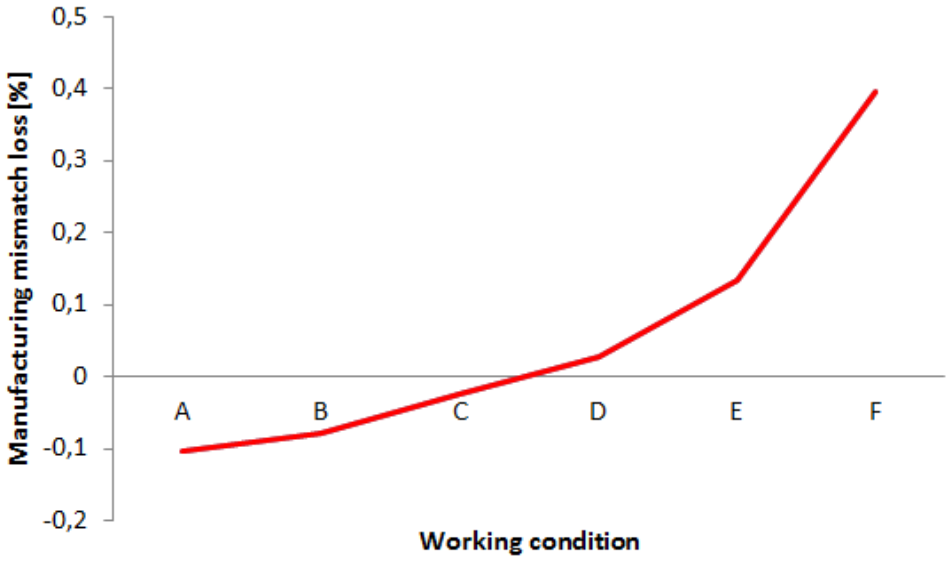

Fig.7. Manufacturing mismatch losses at different working conditions